DIRECT NUMERICAL SIMULATION OF TURBULENT FLOW PAST A CYLINDER WITH SPLITTER PLATE

Leonardo Antonio de Araujo, leonardo.araujo@ufrgs.br
Edith Beatriz Camaño Schettini, bcamano@iph.ufrgs.br
Instituto de Pesquisas Hidráulicas, Universidade Federal do Rio Grande do Sul. Av. Bento Gonçalves, 9500 - Porto Alegre, RS, Brasil

Jorge Hugo Silvestrini, jorgehs@pucrs.br
Faculdade de Engenharia, Pontifícia Universidade Católica do Rio Grande do Sul, PUCRS. Av. Ipiranga, 6681 - Porto Alegre, RS, Brasil

Abstract. *The splitter plate has been one of the most successful devices in controlling the vortex shedding in the wake of cylinder. In the present work, direct numerical simulations (DNS) of a cylinder with a fixed plate are performed. The Reynolds number chosen was $Re = 1250$ and the splitter plate length was varied up to twice the cylinder diameter. The Reynolds stresses, Strouhal number, turbulent kinetic energy and formation length have been studied in order to determine the effect of the plate on the vortex shedding. The splitter plate was effective in attenuating the turbulence intensity, showing good agreement with experimental data. A reduction of 5% in the vortex shedding frequency was observed in a three-dimensional wake when the splitter plate reaches two diameter length.*

Keywords: *cylinder, splitter plate, vortex shedding, direct numerical simulation*

1. Introduction

Flows around obstacles with different geometries are a common phenomenon in nature, being the smooth circular cylinder a canonical object of study. Despite its geometric simplicity, many complex phenomena take place: transition to turbulence, displacement of the boundary layer, separation and formation of Von Karman vortex street (Tritton, 2005).

There are several applications to study the flow around cylindrical geometries. The process of extracting oil from seabed, for example, is made by floating platforms, equipped with slender tubes called risers that conduct oil from the ocean underground to the platform (Blevins, 2001). These structures are subject to action of ocean currents, waves and the movement of platforms where they are anchored. A consequence of combination of these various phenomena involved is the vortex shedding, which can induce vibrations in these structures (called vortex induced vibrations - VIV), reducing its lifespan. In order to reduce vortex shedding and hence the vibrations, several studies have been conducted and some passive control devices have been proposed (Choi *et al.*, 2008).

In the present work, the passive control device chosen for study is the splitter plate. Its thickness is around one order of magnitude smaller than cylinder diameter and is positioned downstream of cylinder.

Experiments conducted by Roshko (1954), for $Re = 14500$, have shown that the inclusion of a splitter plate of $L/D = 5$ could inhibit the vortex shedding with a significant reduction of the pressure coefficient. When the splitter plate dimensionless length (L/D) is $L/D = 1$, the vortex shedding is not completely attenuated, but the Strouhal number (St) and drag coefficient ($< C_D >$) decrease.

Gerrard (1966) investigated the frequency of vortex shedding in a cylinder with plate length up to $L/D = 2$. It was found the St decreased as L/D increased, and minimum St was observed when $L/D \simeq 1$. Further increase in length of plate resulted in increase of St.

Apelt and West (1973) observed, for Re from 10^4 and 5.10^4, the drag on the cylinder was reduced by stabilizing the separation points of the boundary layer, producing a narrower street. The plate increased the base pressure around 50% and decreased the St number.

Experiments in the range of Re between 140 and 1600 were conducted by Unal and Rockwell (1988). The observed flow patterns observed were divided into two separate regions: pre-vortex formation regime and post-vortex formation regime, characterized, respectively, by the absence or the presence of large-scale vortices upstream of the plate tip.

Nakamura (1996) conducted experiments on bluff bodies with splitter plates to investigate vortex shedding characteristics. The Re range studied was $300 < Re < 5000$ and plate length was varied up to $L/D = 15$. It was found that vortex shedding from bluff bodies with extended splitter plates is characterized by the impinging-shear-layer instability, for which the Strouhal number, based on the streamwise dimension of the bluff body (on this case, the splitter plate length) is weakly dependent on geometry and Reynolds number.

In a two-dimensional numerical simulation of a flow around a cylinder with fixed plate for $Re < 100$, Kwon and Choi (1996) confirmed the continuous decrease of the St number as L/D increased. For $Re > 120$, the authors found a local maximum of St for $L/D = 2$ and then a continuous decrease of St for increasing L/D. It was proposed that an interaction between the secondary vortex formed in the plate and the primary vortex detached from the cylinder is the responsible for the increase of St for small plate lengths.

Ribeiro *et al.* (2004) studied numerically the transitional and laminar regimes in vortex shedding around cylinders with splitter plate. In agreement with the results of Kwon and Choi (1996) for $Re = 100$ and 160, the vortex shedding was reduced when L/D increased with a local maximum at $L/D = 2$ for $Re = 160$. For $Re = 300$, the plate length was varied up to $L/D = 10$, with no suppression of vortex shedding.

Akilli *et al.* (2008) investigated the effect of the splitter-plate on vortex shedding, by varying L/D from 0 to 2.4 through physical experiments using PIV (particle image velocimetry). In this work, the turbulent kinetic energy of flow decreased as the plate length increased.

In the present paper, three-dimensional direct numerical simulation (DNS) have been performed for $Re = 1250$ for $L/D = 0$, 1 and 2. The objective of this paper is to study the influence in the vortex street of a splitter plate placed downstream of a fix cylinder. This paper is summarized as follows. In Section 2 the flow configuration, governing equations and numerical methods are presented. In section 3 validations tests for two-dimensional configurations are developed while the main results for the three-dimensional DNS are discussed. In section 4, final conclusions are given.

2. Flow configuration and numerical methods

The equations of continuity and momentum for an incompressible fluid flow are solved in the domain configuration shown in Fig 1. These equations are used in a dimensionless form based on U (freestream velocity), D (cylinder diameter) and ρ (density). The continuity equation is given by:

$$\vec{\nabla} \cdot \vec{u} = 0, \tag{1}$$

and the Momentum equation

$$\frac{\partial \vec{u}}{\partial t} + \frac{1}{2}[\vec{\nabla}(\vec{u} \otimes \vec{u}) + (\vec{u} \cdot \vec{\nabla})\vec{u}] = -\vec{\nabla}\Pi + \frac{1}{Re}\vec{\nabla}^2\vec{u} + \vec{f}, \tag{2}$$

where Π is the modified pressure field and $\vec{f}$ the external force field representing the immerse obstacle.

Equations 1 and 2 are numerically solved using the code *Incompact3d* (Laizet and Lamballais, 2009), which is based on a compact sixth order finite difference scheme (spatial discretization) and a third order Adams-Bashforth scheme (temporal discretization). The cylinder and the plate are generated in the grid through Immersed Boundary Method (IBM), imposing zero velocity inside the obstacle (Parnaudeau *et al.*, 2007). The computational domain parameters and boundary conditions are shown on Figure 1.

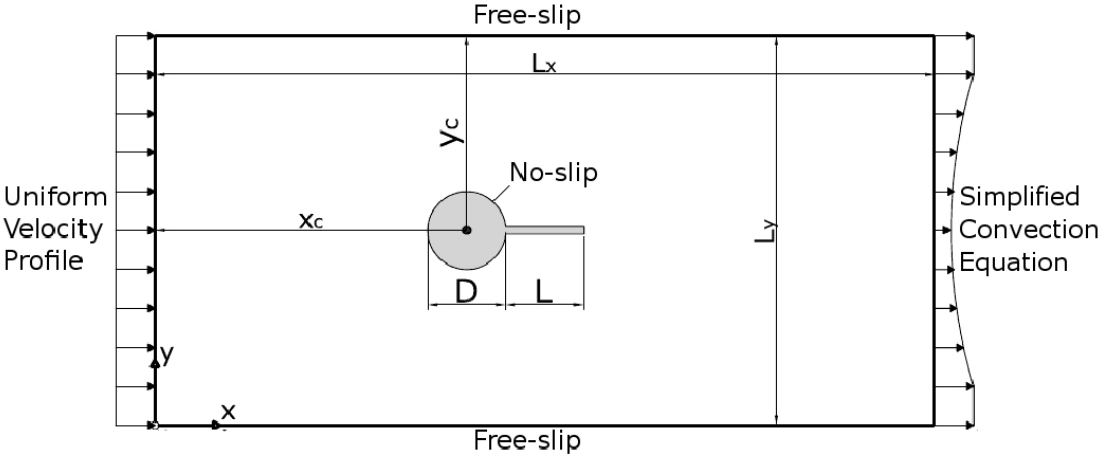

Figure 1. Computational domain parameters and boundary conditions utilized in the present work.

Regarding boundary conditions, at the inlet, a uniform velocity profile $\vec{u} = (1, 0, 0)$ is imposed. The free-slip condition is employed in the lateral borders. At the outlet, a simplified convection equation is utilized.

For identification of coherent structures, it is computed the Q-criterion (Dubief and Delcayre, 2000) defined by:

$$Q = \frac{1}{2}(\Omega_{ij}\Omega_{ij} - S_{ij}S_{ij}), \tag{3}$$

where Ω_{ij} is the rotation rate tensor and S_{ij} the deformation rate tensor. When $Q > 0$, rotation Ω_{ij} dominates shear S_{ij}, indicating a region of coherent vortex.

In this work, the formation length (L_f) is defined as the length, from the cylinder centre, for which the corresponding Reynolds Stress is maximum (Noca et al., 1998).

3. Results

All numerical simulations performed are shown in Table 3. In this table is summarized the main numerical parameters for each 2D and 3D simulations including: the domain dimensions (L_x, L_y, L_z), mesh resolution (n_x, n_y, n_z), time step (Δt), Re number and plate length (L/D). The cylinder center position is placed in $X_C = 8$ and $Y_C = 9$ (Figure 1). An appropriate level of accuracy is reached with a mesh of $\Delta x = \Delta y = 0.0277$ using grid convergence tests.

Table 1. Summary of the numerical parameters

Case	L_x, L_y, L_z	n_x, n_y, n_z	Δt	Re	L/D
I	$20, 18, -$	$721, 649, -$	10^{-3}	100	$0, 0.5, 1, 1.5, 2, 2.5$
II	$20, 18, -$	$721, 649, -$	10^{-3}	160	$0, 0.5, 1, 1.5, 2, 2.5, 3, 3.5, 4, 4.5$
III	$20, 18, 6$	$1081, 973, 128$	8.10^{-4}	1250	$0, 1, 2$

In order to validate the numerical code, 2D simulations for $Re = 100$ and $Re = 160$ (cases I and II) are performed and compared with the numerical work of Kwon and Choi (1996). Good global results are obtained for St (Figure 2) and $< C_D >$ (Figure 3). The maximum relative difference observed, concerning both the $< C_D >$ and St, is approximately 5%.

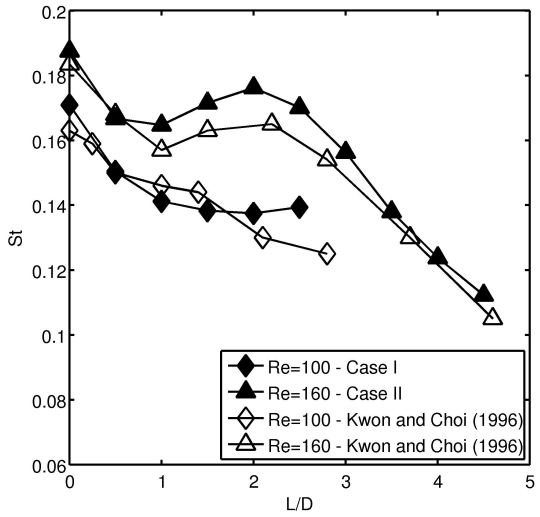

Figure 2. Strouhal number (St) for $Re = 100$ and $Re = 160$.

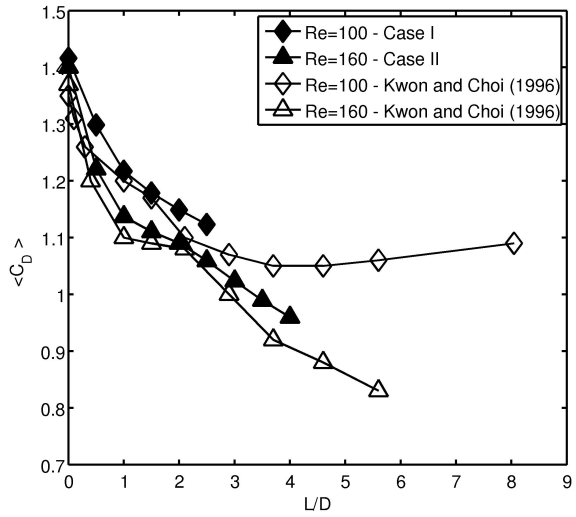

Figure 3. Mean drag coefficient ($< C_D >$).

In the present work, the early subcritic regime for $Re = 1250$, is studied through three-dimensional simulations for $L/D = 0$ (no plate), $L/D = 1$ and $L/D = 2$ (case III). Turbulence statistics such as the Reynolds stresses and formation length are computed and compared with experimental results.

The maximum Reynolds stresses and the corresponding formation lengths are shown in Table 2. For reference, it has been included the data obtained from Noca *et al.* (1998) for $Re = 1260$. The differences obtained may be attributed to the water channel boundary layer effects as commented by the authors (free surface and no-slip at the channel bottom). According to them, these conditions modify the base pressure and consequently the formation length.

The insertion of the plate reduced the absolute value of all stresses and increased formation lengths, moving away from the cylinder the point of stabilization of the wake, where the vortex street is established. These results are in agreement with the experimental work by Akilli *et al.* (2008) for $Re = 6300$.

Table 2. Maximum Reynolds stresses (absolute values) and formation length (L_f)

	$< u'^2 >$	$< v'^2 >$	$< u'v' >$	$L_f(< u'^2 >)$	$L_f(< v'^2 >)$	$L_f(< u'v' >)$
Noca *et al.* (1998) ($Re = 1260$)	0.12	0.32	0.09	2.00	2.61	2.46
$L/D = 0$	0.18	0.35	0.10	1.63	2.30	2.29
$L/D = 1$	0.12	0.30	0.08	2.33	3.24	3.25
$L/D = 2$	0.16	0.25	0.10	2.90	3.80	3.80

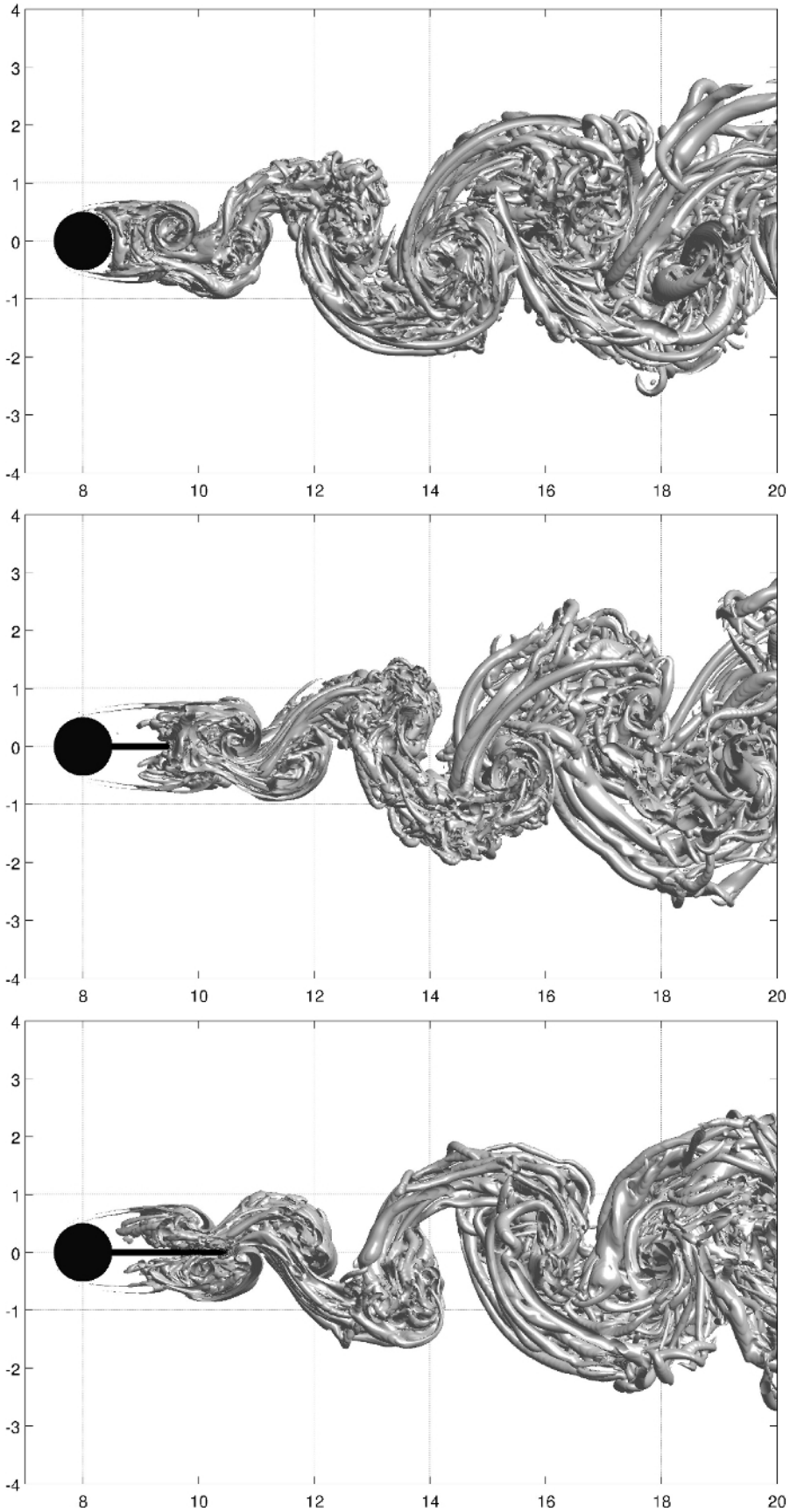

Figure 4. Sideviews of iso-surface of Q-Criterion with the threshold value of $Q = 0.08$ at $t = 108.8$ for $L/D = 0$ (no plate), $L/D = 1$ and $L/D = 2$.

Figure 4 displays side views of the Q-criterion isosurfaces for an isovalue of $Q = 0.08$ of each 3D simulations at $t = 108.8$. For $L/D = 1$, the plate moves away the region of vortices generation. When $L/D = 2$, the vortices are generated alongside the plate. As the plate length increased, the amount of eddies scales observed decreased: the small eddies become less visible and the large eddies decrease in size.

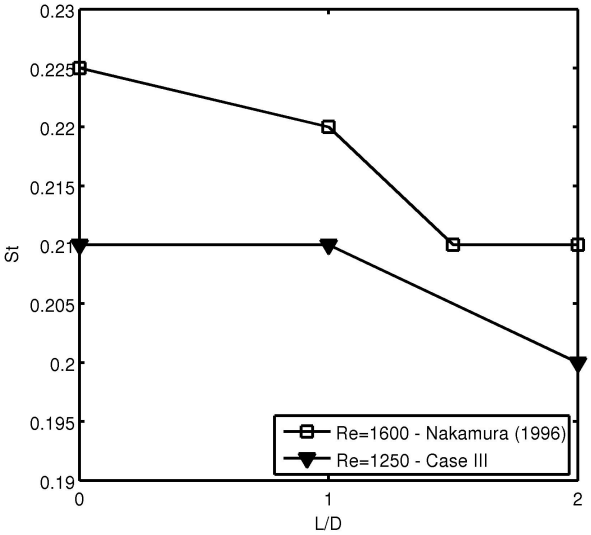

Figure 5. Strouhal number (St).

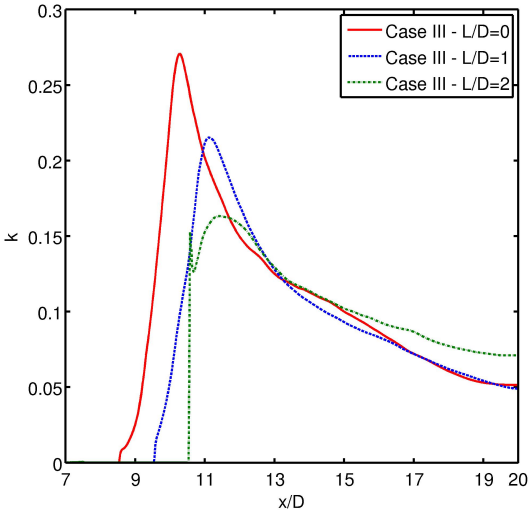

Figure 6. Mean turbulent kinetic energy per mass unit (k).

In Figure 5 is plotted the results for St for $Re = 1250$ as function of L/D alongside the data from Nakamura (1996). For this Re number, the splitter plate has no considerable effect in reducing the St compared to lower Re cases. Nevertheless a decrease of 5% in the St number is found for $L/D = 2$ in agreement with the experimental work of Nakamura (1996).

In Figure 6, the turbulent kinetic energy (k) maximum is moved downstream as L/D increase. This result may be linked to the increase of L_f as seen in Table 2. The kinetic energy decreases on the same trend along the wake when $L/D = 1$ and $L/D = 0$ (no plate) for $x/D > 13$. When $L/D = 2$, the curve continues to decrease, but decays in a lower rate when compared to L/D and $L/D = 0$.

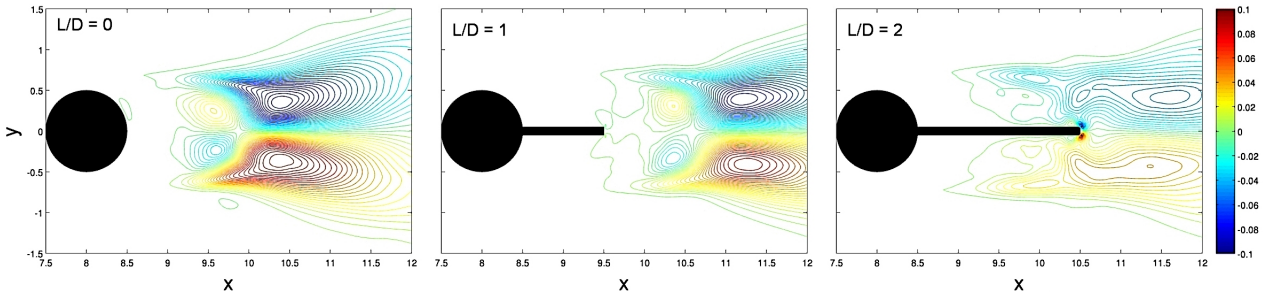

Figure 7. Field of Reynolds Stress $< u'v' >$ for $L/D = 0, 1$ and 2.

For $L/D = 1$, the splitter plate has no considerable effect to modify the stress field configuration (e.g., $< u'v' >$ in Fig. 7) until $L/D = 2$. When $L/D = 2$, the intensity of Reynolds stress at the tip of the plate increases, linked to a decrease in the St (Figure 5). As reported for Re in the laminar regime, for $L/D = 2$, the plate generate a pair of vortices at its tip, increasing energy dissipation as seen through the maximum Reynolds Stresses (Table 2) and the decrease on St number (Fig. 5).

4. Conclusions

Direct numerical simulations (DNS) of flow around a fixed cylinder with splitter plate have been performed in order to study the vortex wake and turbulence statistics. The numerical approach is validated in two-dimensional configuration with maximum difference in order of 5% for the $< C_D >$ and St. Three 3D DNS for $Re = 1250$ are performed and the results are compared with Nakamura (1996), Noca *et al.* (1998) and Akilli *et al.* (2008).

In the case when $Re = 1250$ (3D simulations) the St had no significant attenuation, decreasing to a maximum of 5% for $L/D = 2$, in agreement with the study by Nakamura (1996) for $Re = 1600$. The plate presence attenuated the turbulent kinetic energy in the wake along with the Reynolds Stresses. It was shown that the splitter plate is able of reducing the main turbulence statistics such as kinetic energy and Reynolds stresses for lower Reynolds numbers, in agreement with experimental data by Akilli *et al.* (2008).

5. Acknowledgements

The authors thank the Centro Nacional de Supercomputação (CESUP) on the Universidade Federal do Rio Grande do Sul (UFRGS) and Conselho Nacional de Desenvolvimento Científico e Tecnológico (CNPq) for the financial support.

6. References

Akilli, H., Karakus, C., Akar, A., Sahin, B. and Tumen, N. F. Control of Vortex Shedding of Circular Cylinder in Shallow Water Flow Using an Attached Splitter Plate. Journal of Fluids Engineering 130 (2008).

Apelt, C. J., and West, G. S. The effects of wake splitter plates on bluff-body flow in the range $10^4 < Re < 5.10^4$. Part 1. J. Fluid Mech. 61 (1973), 187-198.

Apelt, C. J., and West, G. S. The effects of wake splitter plates on bluff-body flow in the range $10^4 < Re < 5.10^4$. Part 2. J. Fluid Mech. 71 (1973), 145-160.

Blevins, R. D. Flow Induced Vibration. Van Nostrand Reinhold Co., New York, 2001.

Bloor, M. S., and Gerrard, J. H. Measurements on Turbulent Vortices in a Cylinder Wake. Proc. Roy. Soc. Ser. A. 294 (1966), 319-342.

Choi, H., Jeon, W. and Kim, J.. Control of flow over a bluff body. Annu. Rev. Fluid Mech. 40 (2008), 113-139.

Dubief, Y., and Delcayre, F. On coherent-vortex identification in turbulence. Journal of Turbulence 1 (2000).

Gerrard, J. H. The mechanics of the formation region of vortices behind bluff bodies. J. Fluid Mech. 25 (1966), 25-40.

Kwon, K., and Choi, H. Control of laminar vortex shedding behind a circular cylinder using splitter plates. Phys. Fluids 8 (2) (1996), 476-486.

Laizet, S., Lamballais, E., 2009, High-order compact schemes for incompressible flows: A simple and efficient method with quasi-spectral accuracy, J. Comp. Phys., Vol. 228, pp. 5989-6015.

Lele, S. K., 1992, Compact Finite Difference Schemes with Spectral-like Resolution, J. Comp. Phys., Vol. 103, pp. 16-42.

Nakamura, Y. Vortex shedding from bluff bodies with splitter plates. Journal of Fluids and Structures 10 (1996), 147-158.

Noca, F., Park, H. G., and Gharib, M. Vortex formation length of a circular cylinder ($300 < Re < 4000$) using DPIV. ASME Fluids Engineering Division Summer Meeting. (Washington, DC, 1998), pp. 1-7.

Parnaudeau, P., Heitz, D., Lamballais, E. and Silvestrini, J. H. Direct numerical simulations of vortex shedding behind cylinders with spanwise linear nonuniformity. Journal of Turbulence Vol. 8, No. 13 (2007).

Roshko, A. On the drag and the shedding frequency of two-dimensional bluff bodies. NACA TN 3169 (1954).

Tritton, D. J. Physical Fluid Dynamics. Clarendon Press, Oxford, 2005.

Unal, M. F., and Rockwell, D. On vortex formation from a cylinder. part 1. the initial instability. J. Fluid Mech. 190 (1988), 491-512.

Unal, M. F., and Rockwell, D. On vortex formation from a cylinder. part 2. control by splitter-plate interference. J. Fluid Mech. 190 (1988), 513-529.

7. Responsability notice

The authors are the only responsible for the printed material included in this paper.